



Performance analysis of screw turbine with varying design parameters

Pawan khalal^a, Swarnim Duwadi^{a,*} and Abhishek Pandey^a

^aDepartment of Automobile and Mechanical Engineering, Thapathali Campus, Tribhuvan University, Nepal

ARTICLE INFO

Article history:

Received 29 August 2024

Revised in 6 October 2024

Accepted 20 October 2024

Keywords:

Archimedes Screw Turbine

ANSYS

CFD

Blades

Flow rate

Abstract

Small hydropower plays a crucial role in sustainable development, especially in rural areas of developing countries, by offering a cost-effective, local energy solution. This project focuses on optimizing Archimedean Screw Turbines (ASTs) through the analysis of key design variables: flow rate, inclination angle, and blade count. Evaluating twelve AST configurations across two flow rates (0.153 m³/s and 0.210 m³/s), three inclination angles (22.5, 24.5, and 27 degrees), and two blade setups (two and three) under a 4m head, we discovered optimal performance metrics. The three-blade model at a 24.5-degree angle and 0.210 m³/s flow rate achieved the highest efficiency of 75.38% and a torque of 1694.834 Nm, outperforming the two-blade configurations. Thus, the ideal AST design for boosting small hydropower efficiency is a three-bladed turbine at a 0.210 m³/s flow rate and 24.5-degree inclination, heralding a significant advancement for renewable energy access in remote communities.

©JIEE Thapathali Campus, IOE, TU. All rights reserved

1. Introduction

In the evolving landscape of renewable energy technologies, the quest for efficient, sustainable, and environmentally friendly power generation methods has led to a resurgence in the exploration of traditional mechanisms adapted for modern applications. Among these, the Archimedean Screw Turbine (AST), a device with ancient roots, has emerged as a promising contender, especially in the realm of low-head hydropower generation. The simplicity of its design, coupled with its versatility and minimal ecological footprint, makes AST an attractive option for energy harvesting from water sources with relatively low hydraulic heads.


The principle of the AST is straightforward yet ingenious: it converts the potential energy of water into mechanical energy through the rotation of a helical screw within an inclined cylindrical shaft. As water flows over the blades of the screw, it imparts rotational force, turning the screw and the shaft connected to a generator, thereby producing electricity. This simple operation belies the complex interplay of physical parameters that

govern the efficiency and effectiveness of energy conversion within the system. Among these parameters, the number of blades on the screw, the rate of water flow, and the inclination angle of the turbine stand out as critical factors influencing the AST's performance.

Recent studies, including those by researchers like Kashyap et al. (2020) and Dellinger et al. (2016), have underscored the importance of these variables in the operational efficiency of ASTs. Investigations have revealed that the design and configuration of these parameters can significantly impact the turbine's ability to convert water flow into mechanical energy [1][2]. For instance, Lyons (2014) explored the effect of increasing the number of blades on the screw, revealing that while additional blades can enhance the turbine's torque output, there is a threshold beyond which further additions yield diminishing returns on efficiency [3]. This suggests an optimal blade count that maximizes energy conversion without unnecessarily complicating the turbine's design or increasing its manufacturing costs.

The flow rate of water through the turbine represents another pivotal factor. As the volume of water interacting with the screw increases, so does the potential for energy generation. However, this relationship is not linear. Lashofer et al. (2012) demonstrated that beyond

*Corresponding author:

 swarnim.074bme044@tcioe.edu.np (S.D.)

certain flow rates, the efficiency of ASTs begins to decline, likely due to the onset of hydraulic losses and the turbine's reduced capacity to manage higher volumes of water efficiently [4]. This finding points to the need for balancing flow rate with the physical capabilities of the turbine to ensure optimal performance.

Perhaps the most intriguing parameter is the inclination angle of the turbine. The work of Edirisingh et al. highlights the significance of this factor, noting that while lower inclination angles are commonly used to maintain high efficiency levels, they necessitate longer screws, which can introduce structural complications such as bending problems and bearing constraints [5]. Their research found that an inclination angle of 45 degrees allowed for maximum efficiency, challenging conventional design norms, and suggesting a nuanced relationship between the turbine's angle and its operational efficiency.

This paper aims to build upon these insights, offering a comprehensive analysis of the performance characteristics of ASTs across varied configurations of blade numbers, flow rates, and inclination angles. By synthesizing findings from Computational Fluid Dynamics (CFD) simulations, we seek to map the efficiency landscape of ASTs, identifying design configurations that optimize energy extraction. Through this approach, we hope to illuminate the pathways through which AST technology can be refined and optimized for broader application in renewable energy systems.

2. Literature review

In his 2000 paper, C. Rorres detailed the optimization of the Archimedean screw, distinguishing between its internal (inner radius, blade number, and pitch) and external (outer radius, length, slope) features [6]. He proposed a MATLAB-based method for optimizing design through the radius ratio, pitch ratio, and volume-specific ratio. The study found the theoretical turbine efficiency to be lower than observed in experiments, attributing the discrepancy to unaccounted losses in the theoretical model [6].

In their 2017 study, A. Nuramal et al. explored the performance of a screw turbine under a 0.25m head and a 1.2 l/s flow rate across three different inclination angles, adjusting water head to test variations [7]. At a 22-degree inclination angle, their model produced 1.4W of electricity at 49% efficiency. This single-bladed screw turbine, with a diameter of 0.142 meters, demonstrated that torque output decreased as the inclination angle and rpm increased, providing valuable insights into the operational dynamics of screw turbines under varying conditions [7]. M. Lyons' 2014 study revealed that turbine performance slightly decreases with more than three

blades and significantly with fewer than two. Efficiency increases with diameter until a critical threshold, peaking with a pitch ratio near 1.6. Beyond a pitch ratio of 2.4, efficiency declines. The study highlighted that this efficiency drop-off point varies among Archimedean screw turbine designs, suggesting a complex interplay between design factors and performance [3].

A. Dragomirescu and M. Schiaua's 2017 research devised a method for optimizing the design of Archimedean Screw Turbines (AST) by focusing on maximizing torque output [8]. This approach involves estimating the water bucket volume between blades—a crucial factor without a direct analytical formula—thus initially approximated and later refined through regression analysis of high-efficiency turbines. Additionally, they determined rotational speed based on the turbine's ability to handle its rated discharge at this optimal speed, providing a practical framework for enhancing AST design and performance.

In their 2020 and 2021 study, K. Shahverdi et al. explored the potential of Archimedean Screw Turbines (AST) to generate energy at very low heads, utilizing CFD for performance analysis across variables such as screw speed, flow rates, and inclination angles. The AST's numerical model was validated against experimental data, achieving a minor relative inaccuracy of 0.69% under specific conditions. Key findings include mechanical power increasing with rotational speed up to an optimal point, beyond which it declines. Optimum efficiency was observed when water entry was just below the screw's top inner diameter, with overflow leakage at higher levels reducing efficiency. The study determined that mechanical power peaks at a 30-degree inclination, with efficiency improving alongside rotational speed. However, efficiency peaks at 80% and 83% for flow rates of 1.13 l/s and 1.51 l/s, respectively, at a 24.9-degree angle, making 24.5 degrees the ideal construction angle. This research highlights the capability of ASTs to maintain efficiency with a flow variance of about 20%, marking a significant advance in optimizing AST design and operational parameters [9][10].

In their 2016 study, C.Z. Rosly et al. focused on optimizing screw turbine design for maximum efficiency, experimenting with the number of helix turns and turbine blades to reduce production costs. Utilizing CFD under constant boundary conditions with isentropic and isothermal temperatures in steady state flow, they investigated the water's streamline to determine turbine efficiency. Their findings indicated that reducing the helix's number of turns enhanced turbine performance, with the optimal configuration being 3 helix turns and 3 blades, achieving an 81% efficiency. The study suggested that the variations in helix and blade numbers alone were not conclusive, recommending adjustments

in other design parameters like inclination angle and length for comprehensive efficiency analysis. They advocated for examining these parameters under steady-state conditions to gain more accurate insights into their effects on turbine efficiency [11].

G. Muller & J. Senior's 2009 study highlighted that the power generated by a screw turbine stems from the water's tangential velocity as it moves over the screw blades, not merely its weight. Their research, which didn't account for gap losses, indicated that static force due to the head difference across the blades and the tangential component of this force are critical for screw rotation. Efficiency, they found, is primarily determined by the turbine's geometry rather than its speed, with optimal efficiency closely linked to the screw's design, including blade shape, number of rotations, inclination angles, inflow depth, and radius. Notably, efficiency reaches only about 50% when the screw is not fully engaged, underscoring the influence of blade geometry and the balance between inflow depth and radius on performance. The study concludes that maximum efficiency is contingent upon minimizing leakage losses and optimizing blade geometry [12].

In their 2012 study, A. Lashofer et al. delved into the construction and operational dynamics of Archimedean Screw Turbines (AST), consulting various manufacturers to understand design factors affecting turbine performance. They analyzed multiple variables, including flow rates, water level variations, and the turbines' working head, alongside monitoring screw rotational speed and electrical output under steady-state, constant flow conditions. Efficiency metrics were primarily linked to electrical power generation, with flow rates investigated ranging from 0.25 to 5 m³/s and a common pitch to outer diameter ratio of 1. The study found generator outputs between 4 to 140 kW, with peak efficiencies around 75% and overall measured efficiencies at 69%. The discrepancy was attributed to suboptimal rotation speeds for given discharges. Their findings suggest that efficiency decreases with partial loads due to increased gap losses and at higher loads from spillover inside the screw, indicating the need for optimizing rotational speeds and load management for improved AST efficiency [4].

In their 2016 study, J. Rohmer et al. aimed to optimize plant arrangements for specific sites by incorporating real-world environmental factors into electromechanical system models. They analyzed key variables like inner and outer radii, thread pitch, blade count, and inclination angle, finding the typical usage of Archimedes screw turbines to span heads of 1 to 6.5 meters and flows from 0.25 to 6.5 m³/s. The power output ranged from 1.7 to 300 kW, achieving an overall efficiency of 72%. Utilizing size charts from Rorres and Numberk to pinpoint ideal geometric traits, their model accounted

for various losses such as leakage, overflow, and friction. They highlighted the critical impact of rotational speed and water volume on the turbine's mechanical torque, emphasizing that torque is directly influenced by how much the screw is filled. The study noted that most inaccuracies in predictions stemmed from hydraulic factors and overlooked friction losses in the upstream basin, concluding that accounting for these losses is crucial for enhancing turbine efficiency and design [13].

In their 2020 study, K. Kashyap et al. explored the use of screw turbines in the Himalayan regions of India, employing three different turbines with varying pitches made from stainless paint-coated steel for smoother operation. Their findings indicated a decrease in efficiency as flow rates increased, with the highest efficiency (70.02%) observed at a flow rate of 1 l/s and 68 rpm. Efficiency declined with an increase in inclination angle due to spillage and friction, yet improved with pitch increases, peaking at a pitch of 0.3 meters. The study also noted that power output generally rose with inclination up to a 45-degree angle, beyond which it decreased due to losses. RPM increased with both inclination angle and pitch until reaching a threshold at 45 degrees, attributed to increased spacing between blades allowing quicker bucket filling. The experimental data were validated against theoretical formulas, highlighting key dynamics between pitch, inclination angle, flow rate, and efficiency in screw turbines [2].

An experiment by T. Saroinsong et al. in 2016 revealed that the vortex and bubble phenomena between the blades is caused by the momentum of the hydrostatic force toward the blade and impacts the angular momentum of the turbine shaft in two opposed directions. By lowering the slope of the turbine shaft, one may lessen the vortex's ability to draw kinetic energy from the turbine shaft, which reduces power. At a flow rate of 0.5 m/s, an inclination angle of 25 degrees, and an axial transport velocity of 0.11 m/s, the efficiency was at its highest. 89% efficiency was the maximum [14].

In their 2016 research, G. Dellinger et al. introduced a method to predict Archimedean Screw Turbine (AST) performance through CFD, using a scale model at INSA Strasbourg's fluid mechanics lab under various flow conditions. Their findings revealed that CFD could effectively model overflowing and gap leakages, demonstrating that AST efficiencies exceed 80% across different hydraulic scenarios. The study concluded that ASTs maintain high efficiency within a 20% discharge variation around the optimal value, with minor discrepancies between numerical predictions and experimental results [1].

Dylan Sheneth Edirisingh et al. explored AST performance and flow dynamics, notably at high inclination

angles. While low angles are common for efficiency above 80%, these can lead to lengthy screws with potential bending and bearing issues. Their design reached peak efficiency of 82.1% at a steep 45-degree angle, achieving a notable 9.7 kW power output from a torque of 1695 Nm under a fixed head of 5.2m and flow rate of 0.232m³/s [5].

In their 2016 study, U. Kumar, P. Singh, and A. Tiwari analyzed the performance of a screw turbine installed by Jash Engineering Limited in Indore, India, to assess its suitability for micro-hydro power generation. Despite a potential hydraulic capacity of 29.43KW based on a 5m head and a flow rate of 0.6m³/s, the turbine produced 19.5KW, indicating efficiency losses likely due to design factors. With the turbine set at a 30-degree inclination, tests across flow rates of 0.4m³/s, 0.5m³/s, and 0.6m³/s demonstrated that power output increased with higher discharge, achieving maximum efficiency and a 19.5KW output at the highest flow rate and an operating speed of 3.927 rad/sec. This study highlights that both power output and operational speed of the screw turbine are positively correlated with discharge levels, underscoring the importance of optimizing flow rates and turbine design for enhanced power generation efficiency [15].

While existing studies on ASTs have extensively explored individual design parameters—such as blade number, flow rate, and inclination angle—there remains a significant gap in our understanding of how these variables interact holistically to influence overall turbine efficiency and torque production. Research to date has largely analyzed these factors in isolation, without fully addressing their combined effects on the AST's performance. This oversight leaves a critical void in optimizing AST design for maximum efficiency and operational effectiveness, particularly in adapting to varying parametric conditions. Addressing this gap by investigating the synergistic effects of design parameters on AST efficiency and torque could unlock new pathways for enhancing turbine performance and energy output.

3. Research methodology

3.1. Design and simulations

3.1.1. Screw design

The outer diameter D_o and length L are usually fixed on the basis of the location of the installation of screw turbine. Therefore, these are also known as site parameters. In this study we have assumed this property on the basis of the operating range of the screw turbine from the standard chart.

The angle of inclination of the screw with respect to the horizontal, denoted by the symbol, determines the

slope K . Typically, the head at the installation site is used to determine the value of K . The geometry of the screw is thus defined by the parameters such as internal diameter D_i , number of blades N , pitch of one blade Λ , and gap width. According to C. Rorres, the geometry of the screw turbine is the function of dimensionless parameters such as the volume ratio v [6]. The volume of water in one cycle of the screw V_T , to the total volume of one cycle of the screw $\pi R_o^2 \Lambda$. This has been expressed as:

$$v = \frac{V_T}{\pi R_o^2 \Lambda} \quad (1)$$

Here, R_o is the outer radius and the volume ratio v is a number between 0 and 1. The radius ratio is expressed as:

$$\rho = \frac{R_i}{R_o} \quad (2)$$

The radius ratio is also a dimensionless term between 0 and 1.

The pitch ratio is expressed as:

$$\lambda = \frac{\Lambda \tan \theta}{\pi D_o} \quad (3)$$

The pitch ratio is also a dimensionless term between 0 and 1.

From equation 1, 2 and 3 we get

$$V_T = \frac{2\pi^2 R_o^3}{K \lambda v} \quad (4)$$

From equation 4, the outer radius can be calculated.

Here, the expression for V_T can be written as

$$V_T = \frac{Q}{\text{RPM}} \times 60 \quad (5)$$

The head of the turbine is related to the inclination angle by the following relation.

$$L = \frac{\pi}{\sin \theta} \quad (6)$$

Hence from the inclination angle the length of the turbine can be estimated. The value of V_T , R_o and λ , v can be found from the Rorres's chart of optimized screw parameters [6].

The expression for the pitch of the screw can be expressed in terms of the pitch ratio as:

$$\lambda = \frac{2\pi R_o \lambda}{K} \quad (7)$$

The number of turns of the blade is expressed as:

$$n = \frac{l}{\Lambda} \quad (8)$$

The max rpm of the turbine is calculated as:

$$\text{RPM}_{\max} = \frac{50}{d_o^{2/3}} \quad (9)$$

Figure 1 shows the screw profile generated using the data for pitch and number of revolutions of the screw obtained by using the data in Table 1.

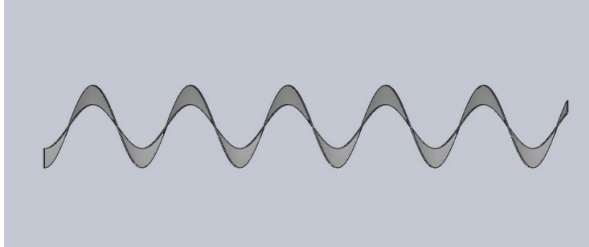


Figure 1: Screw Profile

The “chute” of the screw is the region between two successive flights and its inner radius and outer radius. A screw with N flights has N chutes. The term “bucket” is used to refer to one of the maximally connected regions occupied by the trapped water within any one chute when the water is up to the optimal filling point F . The volume of such a bucket will be denoted by V_B . Figure 2 shows the screw bucket in a screw turbine. The screw profile is mounted on the shaft. The shaft of the desired length is calculated on the basis of the inclination angle of the site.

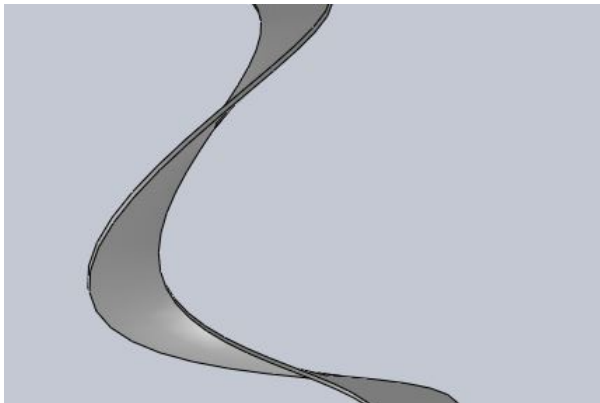


Figure 2: Screw bucket

3.1.2. Design parameters and design of experiment

Flow rate is a crucial parameter in screw turbine design, impacting various performance metrics. The operational flow rate range spans from 0.1 to 50 m³/s, with the most efficient range being 0.1 to 10 m³/s, determined by design considerations and material constraints [16].

A key design challenge is ensuring the turbine can effectively handle incoming flows. Increasing flow rates typically boost power and efficiency, but the added water mass also influences the blade momentum, affecting efficiency across different blade counts [17]. This interplay between flow rate and turbine design underscores the need for careful consideration of flow dynamics in optimizing turbine performance.

Length is also another important parameter in the study of screw turbines this parameter is generally dependent on the slope of the installation site. So, it is a coupled parameter generally depending on the angle of inclination of the site where the screw turbine is to be installed. Generally, installing the turbine on the sites with a low inclination angle results in a longer shaft than that of installation on a site of a higher inclination angle [17]. The head and other parameters change has also to be considered when choosing the length of the shaft.

Lower inclination angles is usually characterized by higher power produced. Low inclination angles between 10-40 degrees are recommended for the installation of a screw turbine. Optimal power production can be achieved in this range. G. Dellinger, et.al., suggest that the installation of the screw must be made between 20-25 degrees for the highest efficiency [18].

The efficiency of screw turbine usually increases on increasing the outer diameter, however on increasing the diameter while keeping other dependent parameters constant. The effect was a decrease in the overall efficiency of the screw turbine. The reason for this is that upon holding the other parameters constant, increasing diameter resulted in lower bucket fill and thus the contribution to torque is also less [19]. The gap also increases with the increase in the diameter and thus the efficiency decrease due to the increase in the leakage loss.

Diameter Ratio is another crucial factor in the design of a screw turbine. The ratio of inner diameter to the outer diameter is the diameter ratio numerically. The general effect is that on decreasing the diameter ratio the torque produced decreases [20]. The blade surface increases as the diameter ratio decrease due to an increase in outer diameter which should increase the efficiency at least theoretically. But the experimental result shows that this does not happen. Upon decreasing the diameter ratio, the volume of the bucket also decreases, and hence runner speed can be increased but it can only be increased so much before the water splashing starts decreasing the efficiency. C. Rorres, (2000) has given the optimized value of diameter ratio for different blade numbers, which is used as the initial assumption for the design of a screw turbine [6].

The pitch ratio has a significant effect on the performance of the screw turbine. For obtaining high per-

Table 1: Parameter values for different experiments

SN	Head (H, m)	Flow (Q, m ³ /sec)	Angle (θ)	Length (L, m)	Outer Radius (R _O , m)	Inner Radius (R _i , m)	Pitch (λ)	Blade
1	4	0.153	22.5	10.4525	0.532	0.2856	1.503	2
2	4	0.21	22.5	10.4525	0.591	0.3174	1.671	2
3	4	0.153	24.5	9.6457	0.549	0.2949	1.411	2
4	4	0.21	24.5	9.6457	0.610	0.3277	1.568	2
5	4	0.153	27	8.8108	0.570	0.3060	1.310	2
6	4	0.21	27	8.8108	0.633	0.3401	1.455	2
7	4	0.153	22.5	10.4525	0.505	0.2706	1.699	3
8	4	0.21	22.5	10.4525	0.561	0.3007	1.888	3
9	4	0.153	24.5	9.6457	0.521	0.2793	1.594	3
10	4	0.21	24.5	9.6457	0.579	0.3104	1.771	3
11	4	0.153	27	8.8108	0.541	0.2899	1.480	3
12	4	0.21	27	8.8108	0.601	0.3222	1.644	3

formance of screw G. Nagel, (1968) suggested that the pitch ratio be greater than 1.6 times the outer radius and below 2.4 [19]. From many experiments, it has been shown that the pitch ratio is chosen below 2 as it produced the most efficiency. But the pitch depends on the number of blades also and thus the volume also increases as the pitch ratio increases. This may have negative consequences while keeping it low may lead to underfilling of buckets. So, the pitch ratio can only be increased up to a limit before the efficiency starts to decrease. It has been shown by M. Lyons (2013) experimentally [20].

As the no of blades increases the weight of the turbine increases, so lower no blades are generally preferred during the design. Choosing a larger no of blades for the turbine also increases the bearing loads thus increasing the bearing losses. The optimal blade number from several experiments has been concluded to be three [20]. However, an experiment performed by G. Dillinger, et. al., (2018) shows that the five-bladed screw generated the highest power among four-bladed and three-bladed [18].

The design rpm of the screw turbine depends on the outer diameter. T. Saroinsong, et. al., (2016) noticed that the highest efficiency occurs at 89% at an rpm of 50 rpm. This is also supported by lower inclination angles of the shaft. The low inclination angle with less rpm of the blades produces the maximum efficiency [21].

Based on these studies, the experiment is designed with the parameter values shown in Table ??.

3.1.3. Computational analysis

The screw geometries were created using a combination of two CAD software packages Solid works and ANSYS Design Modeler. The turbine was first modeled using Solidworks while Ansys Design Modeler

was used to create the cylindrical inlet and outlet section of the turbine. The modeled turbine was subtracted to create an empty space or cavity within the geometry which will represent the turbine in further analysis. The remaining geometry was subdivided into continuous geometric space called mesh which are used as discrete local approximations of the larger domain. The fluid simulation was done in Ansys which works by solving various Navier-Stoke's equations in small meshes. The Navier-Stoke's continuity equation is shown in equation (10), momentum equations in equations (11), (12) and (13) while equation (14) shows the energy equation of Navier-Stoke's equation.

$$\frac{\partial \rho}{\partial t} + \frac{\partial(\rho u)}{\partial x} + \frac{\partial(\rho v)}{\partial y} + \frac{\partial(\rho w)}{\partial z} = 0 \quad (10)$$

$$\begin{aligned} \frac{\partial(\rho u)}{\partial t} + \frac{\partial(\rho u^2)}{\partial x} + \frac{\partial(\rho uv)}{\partial y} + \frac{\partial(\rho uw)}{\partial z} \\ = -\frac{\partial p}{\partial x} \\ + \frac{1}{\text{Re}} \left(\frac{\partial \tau_{xx}}{\partial x} + \frac{\partial \tau_{xy}}{\partial y} + \frac{\partial \tau_{xz}}{\partial z} \right) \end{aligned} \quad (11)$$

$$\begin{aligned} \frac{\partial(\rho v)}{\partial t} + \frac{\partial(\rho uv)}{\partial x} + \frac{\partial(\rho v^2)}{\partial y} + \frac{\partial(\rho vw)}{\partial z} \\ = -\frac{\partial p}{\partial y} \\ + \frac{1}{\text{Re}} \left(\frac{\partial \tau_{xy}}{\partial x} + \frac{\partial \tau_{yy}}{\partial y} + \frac{\partial \tau_{yz}}{\partial z} \right) \end{aligned} \quad (12)$$

$$\begin{aligned} & \frac{\partial(\rho w)}{\partial t} + \frac{\partial(\rho u w)}{\partial x} + \frac{\partial(\rho v w)}{\partial y} + \frac{\partial(\rho w^2)}{\partial z} \\ &= -\frac{\partial p}{\partial z} \\ &+ \frac{1}{\text{Re}} \left(\frac{\partial \tau_{xz}}{\partial x} + \frac{\partial \tau_{yz}}{\partial y} + \frac{\partial \tau_{zz}}{\partial z} \right) \end{aligned} \quad (13)$$

$$\begin{aligned} & \frac{\partial E_T}{\partial t} + \frac{\partial(u E_T)}{\partial x} + \frac{\partial(v E_T)}{\partial y} + \frac{\partial(w E_T)}{\partial z} \\ &= -\frac{\partial(u p)}{\partial x} - \frac{\partial(v p)}{\partial y} - \frac{\partial(w p)}{\partial z} \\ &+ \frac{1}{\text{Re}} \left[\frac{\partial}{\partial x} (u \tau_{xx} + v \tau_{xy} + w \tau_{xz}) \right. \\ &+ \frac{\partial}{\partial y} (u \tau_{xy} + v \tau_{yy} + w \tau_{yz}) \\ &+ \left. \frac{\partial}{\partial z} (u \tau_{xz} + v \tau_{yz} + w \tau_{zz}) \right] \\ &- \frac{1}{\text{Re} \cdot \text{Pr}} \left(\frac{\partial q_x}{\partial x} + \frac{\partial q_y}{\partial y} + \frac{\partial q_z}{\partial z} \right) \end{aligned} \quad (14)$$

Where ρ is the density in kg/m^3 , t is time, u , v , and w are the velocity in the x , y , and z directions. Also, p is the pressure in (Pa), E_T is the thermal energy component, Re is the Reynolds number, τ is the stress, q is the heat flux, and Pr is the Prandtl number.

Although predicting how turbulent fluctuations would impact the flow is a challenging problem that has not yet been fully mastered or understood, it is necessary in practically all engineering fluid flow models. It is crucial to describe turbulence as correctly as possible since it is a dominating phenomenon that, when it occurs, has a significant impact on other phenomena. It is crucial to select the turbulence model that is best appropriate for the project since each model has advantages and disadvantages. The k-epsilon realizable model with wall treatment was the turbulence model that was employed.

3.1.4. Mesh quality

Mesh quality is crucial for accurate simulations, and metrics like skewness and orthogonal quality are key indicators of mesh quality. Skewness measures how much a cell deviates from the ideal shape, with values ideally below 0.9 to ensure quality [22]. In this context, skewness values of 0.864 for two-blade turbines and 0.856 for three-blade turbines suggest a high-quality mesh. Orthogonal quality, assessed through the alignment of face normal vectors with vectors connecting element centers to adjacent elements, ranges from 0 (best) to 1 (worst), with values above 0.1 considered acceptable for maintaining mesh integrity[22]. Here, the orthogonal qualities were 0.2134 for two-blade turbines and

0.2098 for three-blade turbines, both exceeding the minimum threshold and indicating superior mesh integrity. These metrics collectively affirm the mesh's quality for accurate computational simulations. Figure 3 shows the cross-sectional view of Mesh while the Figure 4 shows enlarged cross sectional view of the mesh.

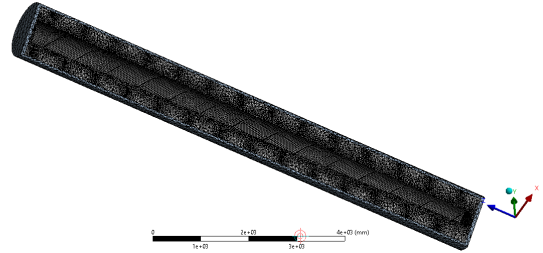


Figure 3: Cross sectional view of Mesh

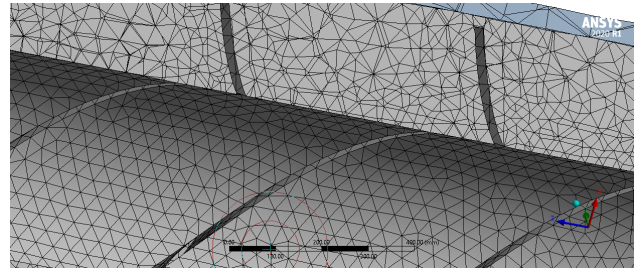


Figure 4: Enlarged Cross sectional view of Mesh

To test the mesh independency, four mesh configurations with element counts ranging from approximately 0.3 to 0.85 million were studied. Despite differences in size, all meshes were generated using the same methods and boundary conditions, focusing on the critical area where fluid meets turbine blade. This ensured that reductions in mesh size directly impacted the area of interest. Each configuration maintained acceptable skewness and orthogonal quality values, demonstrating that even as mesh complexity varied, key quality metrics were consistently met. This approach allowed for a detailed examination of mesh impacts on flow dynamics, ensuring that the area around the turbine blades was accurately represented across different mesh sizes.

Figure 5 illustrates that torque rapidly increases with the number of mesh elements, reaching a plateau at approximately 0.75 million elements. Beyond this point, the increase in torque becomes marginal, particularly between the 0.75 and 0.85 million element meshes, indicating that further increments in mesh size beyond 0.8 million elements yield negligible improvements in results. Consequently, a mesh size of nearly 0.8 million elements was selected for the project, balancing com-

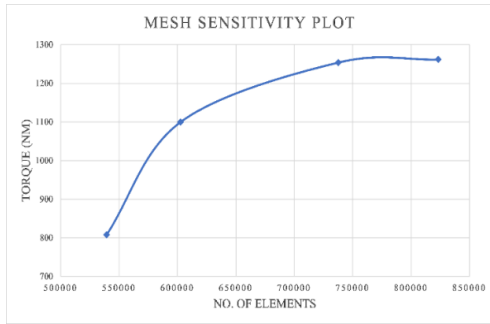


Figure 5: Torque produced for different no. of mesh elements

putational efficiency with accuracy. This decision was informed by the diminishing returns on torque output observed with the finest mesh, where the slight increase in accuracy did not justify the significantly longer computation times.

4. Result and discussion

4.1. Pressure contour

During the study of the pressure contours, the observed behavior aligned with expectations. Figure 6 shows that the pressure at the inlet is significantly high due to the loss of water momentum upon impact with the front portion, effectively creating a high-pressure stationary region. This phenomenon is anticipated as the incoming water abruptly slows down and accumulates, increasing pressure at the point of contact. Consequently, pressure decreases gradually across the blades, a necessary condition for inducing rotation. This gradation in pressure from the inlet to the blades is a critical mechanism that enables the blades to rotate as designed, showcasing the intricate relationship between fluid dynamics and mechanical motion within the turbine system.

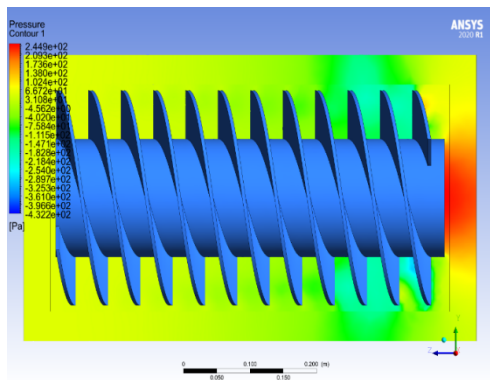


Figure 6: Pressure contour

4.2. Velocity contour

The analysis of the velocity contours reveals that flow leakage is responsible for the higher velocity observed at the turbine tip compared to the shaft which is depicted in Figure 7. This is attributed to the greater distance between the trough and the turbine at the tip, leading to increased velocity in this region. Additionally, as water interacts with the rotating shaft, there's a gradual reduction in velocity within the shaft area. This differential in velocities—higher at the tip and lower near the shaft—is indicative of the complex fluid dynamics at play, where spatial variations within the turbine structure significantly influence the flow characteristics, effectively highlighting the nuanced interplay between structural design and fluid behavior.

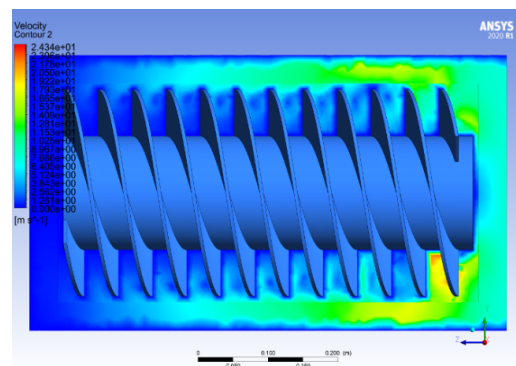


Figure 7: Velocity contour

4.3. Torque and Efficiency

The torque obtained from the results for the simulation for different parameters is shown in the figure below. The torque obtained is the one without the friction effects and other losses.

4.3.1. Torque for three blades at different flow rates

Torque obtained for the 3 bladed turbine at considered flow rates of 0.153m³/s and the 0.210 m³/s at different angles of inclination is shown in Figure 8. As seen in the figure the torque of the 3 bladed turbine at lower flow rate of 0.153m³/s is steadily increasing up to the 27 degrees inclination angle. But for the higher flow rate the torque initially increases up to the inclination angle of 24.5 and then starts decreasing up to 27 degrees. As the flow rate increases the rpm of the blades also increases. As a result of which at the inlet the flow is disturbed and hence the torque produced reduces. Up to 24.5 degrees the effect of decrease in torque is not seen as the flow is easily accumulated in the buckets but after the 24.5 degrees the intake volume of water is disturbed to a limit also overflow losses also occurs. Hence the

torque decreases.

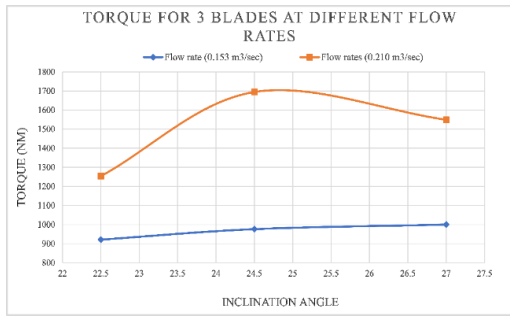


Figure 8: Torque vs. Inclination Angle in degrees for different flow rates for 3 bladed AST

4.3.2. Torque for two blades at different flow rates

The Figure 9 illustrates the torque performance of a two-bladed turbine at varying flow rates (0.153 m³/s and 0.210 m³/s) and angles of inclination. For the higher flow rate of 0.210 m³/s, torque consistently decreases up to a 27-degree inclination angle. Conversely, at the lower flow rate of 0.153 m³/s, torque initially rises until reaching a 24.5-degree inclination, then declines towards the 27-degree mark. This contrast highlights how the turbine’s efficiency and torque output are influenced by the interplay between flow rate and blade inclination, revealing the nuanced dynamics of turbine performance across different operational conditions.



Figure 9: Torque vs. Inclination Angle in degrees for different flow rates for 2 bladed AST

4.3.3. Torque at flow rate of 0.210 m³/sec

The Figure 10 showcases the torque output for two and three-bladed turbines at a uniform flow rate of 0.153 m³/s, analyzed across various angles of inclination. For the three-bladed turbine, torque peaks at a 24.5-degree angle before beginning to decrease. In contrast, the two-bladed turbine demonstrates a continuous increase in torque across all tested inclination angles. This comparison effectively illustrates the distinct performance

characteristics between the two configurations, highlighting how blade count and angle of inclination can significantly influence turbine torque, thereby impacting overall efficiency and operational dynamics.

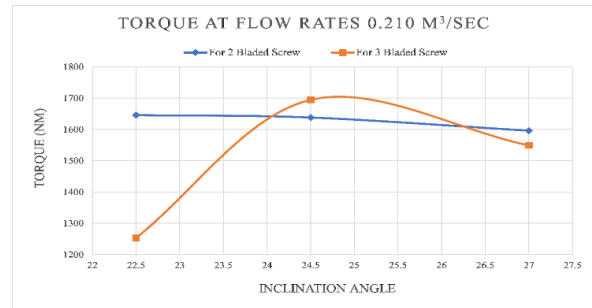


Figure 10: Torque vs. Inclination angle in degrees for different number of blades for 0.210 m³/sec

4.3.4. Torque at flow rate of 0.153 m³/sec

The Figure 11 illustrates torque measurements for two and three-bladed turbines under a constant flow rate of 0.153 m³/s, analyzed at varying angles of inclination. It reveals that for the two-bladed turbine, torque rises until reaching a 24.5-degree angle, after which it begins to decline. Conversely, the three-bladed turbine exhibits a consistent increase in torque across all evaluated inclination angles. This data underscores the impact of blade count and inclination on turbine performance, showing how the three-bladed design maintains a steady improvement in torque, demonstrating its effectiveness over a wider range of operational conditions compared to the two-bladed setup.

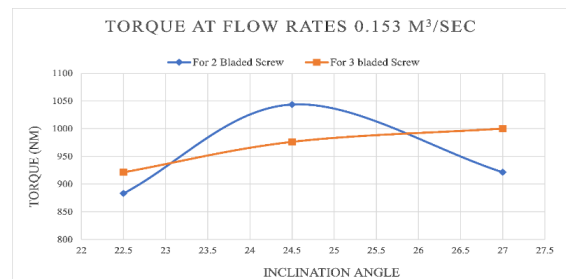


Figure 11: Torque vs. Inclination angle in degrees for different number of blades for 0.153 m³/sec

4.3.5. Efficiency for two blades at different flow rates

The Figure 12 presents efficiency metrics for a two-bladed turbine at flow rates of 0.153 m³/s and 0.210 m³/s, across various inclination angles. It shows that at the higher flow rate of 0.210 m³/s, efficiency consistently declines up to a 27-degree angle. Meanwhile,

at the lower flow rate of 0.153 m³/s, efficiency rises until a 24.5-degree angle, after which it begins to fall, continuing to the 27-degree mark. This pattern mirrors observations from the torque plot, affirming the predictable relationship between flow rate, blade inclination, and turbine performance. The alignment between efficiency and torque trends underlines the influence of operational conditions on turbine output, highlighting how adjustments in flow rate and angle can significantly affect efficiency.

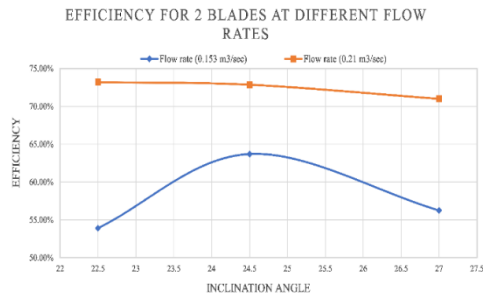


Figure 12: Efficiency vs. Inclination angle at different flow rates for 2 bladed AST

4.3.6. Efficiency for three blades at different flow rates

Figure 13 depicts efficiency curves for a three-bladed turbine, at flow rates of 0.153 m³/s and 0.210 m³/s across varying angles of inclination, illustrate a clear pattern. At the lower flow rate of 0.153 m³/s, the turbine’s efficiency exhibits a consistent rise up to a 27-degree angle. However, at the higher flow rate of 0.210 m³/s, efficiency increases only until reaching a 24.5-degree inclination, beyond which it begins to decline towards the 27-degree mark. This observed efficiency trend mirrors the earlier noted behavior in torque, indicating a direct correlation between the two. Such parallel trends in efficiency and torque affirm the predictability of turbine performance based on flow rate and blade inclination, showcasing the intricate dynamics that govern turbine efficiency.

4.3.7. Efficiency at 0.153 m³/sec

The Figure 14 outlines the efficiency trends for two and three-bladed turbines at a flow rate of 0.153 m³/s across different angles of inclination. For the two-bladed turbine, efficiency peaks at a 24.5-degree angle, beyond which it starts to decline. Conversely, the three-bladed turbine exhibits a consistent increase in efficiency across all tested inclination angles. This comparison highlights the distinct performance advantages of the three-bladed design under the same operational conditions, showcasing its superior ability to maintain efficiency across a

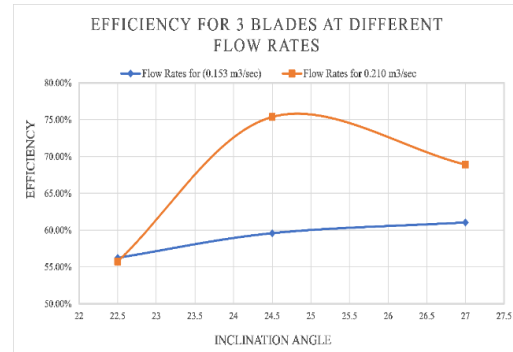


Figure 13: Efficiency vs. Inclination angle at different flow rates for 3 bladed AST

broader range of inclinations. This efficiency behavior underscores the critical role of blade count and angle in optimizing turbine performance, with the three-bladed configuration demonstrating enhanced adaptability and effectiveness.

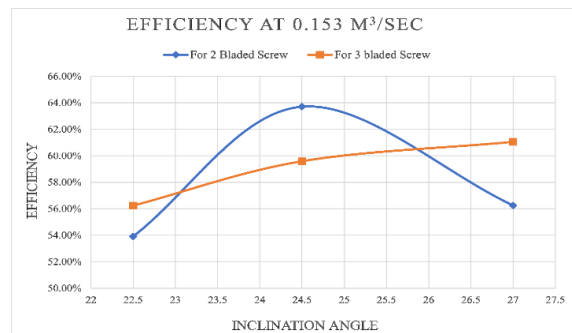


Figure 14: Efficiency vs. Inclination angle at different number of blades for 0.153 m³/sec

4.3.8. Efficiency at 0.213 m³/sec

The efficiency data for two and three-bladed turbines at a flow rate of 0.210 m³/s, presented at varying inclination angles, reveals distinct performance patterns as indicated in Figure 15. The three-bladed turbine shows an increase in efficiency up to a 24.5-degree angle, after which efficiency begins to wane. In contrast, the two-bladed turbine’s efficiency exhibits a consistent decline across all angles of inclination. This contrast underlines the nuanced impact of blade configuration on turbine performance under higher flow conditions, with the three-bladed turbine demonstrating an initial advantage in efficiency that diminishes beyond a certain inclination. Meanwhile, the two-bladed design shows a uniform decrease, emphasizing the importance of blade count and inclination angle in achieving optimal efficiency. This analysis provides insightful guidance on turbine design considerations for maximizing efficiency

under specific operational parameters.

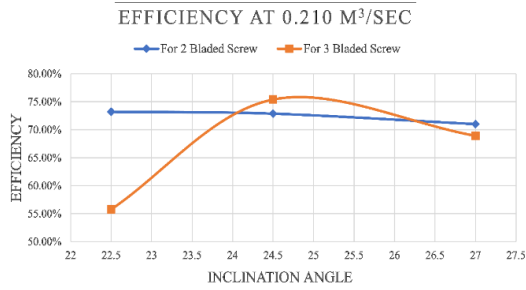


Figure 15: Efficiency vs. Inclination angle at different number of blades for 0.210 m³/sec

At a flow rate of 0.210 m³/sec, the two-bladed screw turbine's efficiency peaks at 22.5 degrees, whereas the three-bladed screw turbine's efficiency reaches its maximum at 24.5 degrees. The highest torque observed for the three-bladed turbine is 1684.834 Nm at a 24.5-degree angle, in contrast to the two-bladed turbine, which achieves a maximum torque of 1646.284 Nm at 22.5 degrees. Notably, both torque and efficiency for the turbines increase with the flow rate.

For the two-bladed turbine, efficiency maximizes at 22.5 degrees, deviating from the initial indication of peaking at 24.5 degrees. Conversely, the peak efficiency for the three-bladed configuration is correctly noted at 22 degrees, with efficiency beginning to diminish after 22.5 degrees. Interestingly, while torque for the two-bladed turbine increases with angle up to 24.5 degrees at a lower flow rate of 0.153 m³/s, it slightly decreases as the angle increases at a higher flow rate of 0.210 m³/s. The three-bladed turbine mirrors this pattern, with torque increasing with the angle at 0.153 m³/s but peaking at 24.5 degrees before decreasing at 0.210 m³/s.

The optimum performance for the two-bladed turbine at 22.5 degrees and 0.210 m³/s results in a maximum torque of 1645.8985 Nm and an efficiency of 73.21%. The three-bladed turbine surpasses this, achieving its best at 24.5 degrees and 0.210 m³/s with a torque of 1694.834 Nm and an efficiency of 75.38%. These findings highlight the nuanced effects of blade number and inclination angle on turbine performance, with both configurations showing varying efficiencies and torque outputs at specific operational conditions.

5. Results validation

Validation stands as a pivotal phase in any modeling or simulation project, essential for affirming the accuracy of results obtained. Our study's credibility was enhanced through validation against an experimental investigation conducted by Lubitz et al. in 2014, which

also guided our approach to simulating the targeted parameters. This experimental benchmark was critical for validating our model's fidelity.

During the model validation process, we recorded a torque measurement of 0.207 Nm, closely aligning with the 0.2 Nm reported by the experimenters. Similarly, our validation efforts yielded an efficiency rate of approximately 69.22%, nearly matching the experimental efficiency of 69%. These minor deviations underscore the reliability of our validation process, indicating a strong correlation between our simulation outcomes and empirical data.

Leveraging the experimenter's model validation approach as a benchmark, we meticulously applied the same rigorous validation standards across all developed models. This methodical approach ensured that our simulation results were not only consistent with, but also comprehensively validated against established experimental findings, thus reinforcing the credibility and accuracy of our research outcomes.

6. Conclusion

The investigation into various geometrical ratios and factors revealed their significant impact on a turbine's performance, culminating in the identification of an optimal design featuring three blades, a 24.5-degree inclination angle, and a flow rate of 210 liters per second (lps). The study observed that efficiency and torque generally increase with the number of blades, inclination angle, and flow rate, yet the benefits plateau beyond a certain point due to increased losses.

Notably, enhancing the mass flow rate consistently improved performance, but limitations in testing variations in length, due to fixed head geometries, highlighted potential areas for future research. The theory suggests that increasing the turbine's length allows for more energy capture from the fluid, although friction forces eventually negate the benefits. A critical length exists where the benefits of increased torque outweigh the frictional losses, beyond which efficiency declines.

The synthesis of favorable design traits into a single geometry demonstrated a notable increase in power and torque output, achieving an efficiency of 75% with a three-bladed turbine at a 24.5-degree angle. This indicates that while optimal efficiency is achievable, all tested geometries produced satisfactory torque and efficiency levels, close to the maximum efficiency observed.

The study underscores the Archimedes screw turbine's viability for low head sites and flows under 1 m³/s, suggesting its potential as a key renewable energy solution. However, to tailor these turbines precisely for energy

generation needs, further research is essential. In contexts where a single turbine's capacity is exceeded, deploying multiple units could offer a scalable solution. The development of screw turbines, especially in regions like Nepal with limited model testing facilities, may significantly contribute to renewable energy advancements in the coming years, underlining the need for enhanced research and development infrastructure.

Ethical statement

This study does not contain any studies with human or animal subjects performed by any of the authors.

Conflicts of Interest

The authors declare that they have no conflicts of interest to this work.

References

- [1] Dellinger G, Garambois P, Dufresne M, et al. Numerical and experimental study of an archimedean screw generator[J]. IOP Conference Series: Earth and Environmental Science, 2016.
- [2] Kashyap K, Thakur R, Kumar S, et al. Identification of archimedes screw turbine for efficient conversion of traditional water mills (gharats) into micro hydro-power stations in western himalayan regions of india: An experimental analysis[J]. International journal of renewable energy research, 2020, 10 (3): 13.
- [3] Lyons M. Lab testing and modeling of archimedes screw turbines[Z]. 2014.
- [4] Lashofer A, Hawle W, Pelikan B. State of technology and design guidelines for the archimedes screw turbine[J]. Proceedings of the Hydro, 2012, 14: 1-35.
- [5] Edirisinghe D S, Yang H S, Kim M S, et al. Computational flow analysis on a real scale run-of-river archimedes screw turbine with a high incline angle[J]. Energies, 2021, 14(11): 3307.
- [6] Rorres C. The turn of the screw: Optimal design of an archimedes screw[J]. Journal of Hydraulic Engineering, 2000, 126(1): 72-80.
- [7] Nuramal A, Bismantolo P, Date A, et al. Experimental study of screw turbine performance based on different angle of inclination[J]. Energy Procedia, 2017, 110: 8-13.
- [8] Dragomirescu A, Schiaua M. Experimental and numerical investigation of a Bánki turbine operating far away from design point[J]. Energy Procedia, 2017, 112: 43-50.
- [9] Shahverdi K, Loni R, Ghobadian B, et al. Numerical optimization study of archimedes screw turbine (ast): A case study[J]. Renewable Energy, 2020, 145: 2130-2143.
- [10] Shahverdi K, Loni R, Maestre J, et al. Cfd numerical simulation of archimedes screw turbine with power output analysis[J]. Ocean Engineering, 2021, 231: 108718.
- [11] Rosly C Z, Jamaludin U K, Azahari N S, et al. Parametric study on efficiency of archimedes screw turbine[J]. ARPN Journal of Engineering and Applied Sciences, 2016, 11(18): 10904-10908.
- [12] Müller G, Senior J. Simplified theory of archimedean screws[J]. Journal of Hydraulic Research, 2009, 47(5): 666-669.
- [13] Rohmer J, Knittel D, Sturtzer G, et al. Modeling and experimental results of an archimedes screw turbine[J]. Renewable Energy, 2016, 94: 136-146.
- [14] Saroinsong T, Soenoko R, Wahyudi S, et al. Fluid flow phenomenon in a three-bladed power-generating archimedes screw turbine[J]. Journal of Engineering Science and Technology Review, 2016, 9(2): 72-79.
- [15] Kumar U, Singh P, Tiwari A. Suitability of archimedes screws for micro hydro power generation in india[J]. International Journal of Thermal Technologies, 2016, 6(3): 273-378.
- [16] YoosefDoost A. Archimedes screw generators and hydropower plants: A design guideline and analytical models[Z]. 2022.
- [17] Yulistiyanto B, Hizhar Y, Lisdiyanti L. Effect of flow discharge and shaft slope of archimedes (screw) turbin on the micro-hydro power plant[J]. 2012.
- [18] Dellinger G, Garambois P A, Dellinger N, et al. Computational fluid dynamics modeling for the design of archimedes screw generator[J]. Renewable Energy, 2018, 118: 847-857.
- [19] Nagel G. Archimedes screw pump handbook: fundamental aspects of the design and operation of water pumping installations using archimedes screw pumps[M]. RITZ-Pumpenfabrik OHG, 1968.
- [20] Lyons M, Lubitz W D. Archimedes screws for microhydro power generation[J]. Energy Sustainability, 2013.
- [21] Saroinsong T, Soenoko R, Wahyudi S, et al. Similarity check: Performance of three-bladed archimedes screw turbine[J]. ARPN Journal of Engineering and Applied Science, 2016, 11(15).
- [22] Inc. A. Ansys fluent tutorial guide[M]. 2022.